# Dynamics of rough surfaces generated by two-dimensional lattice spin models

A. Faissal Brito,[1] José Arnaldo Redinz,[2] and J. A. Plascak[1]
[1]*Departamento de Física, Instituto de Ciências Exatas, Universidade Federal de Minas Gerais, C. P. 702-30123-970, Belo Horizonte, MG, Brazil*
[2]*Departamento de Física, Universidade Federal de Viçosa 36570-000, Viçosa, MG, Brazil*
(Received 11 November 2006; revised manuscript received 19 January 2007; published 9 April 2007)

We present an analysis of mapped surfaces obtained from configurations of two classical statistical-mechanical spin models in the square lattice: the $q$-state Potts model and the spin-1 Blume-Capel model. We carry out a study of the phase transitions in these models using the Monte Carlo method and a mapping of the spin configurations to a solid-on-solid growth model. The first- and second-order phase transitions and the tricritical point happen to be relevant in the kinetic roughening of the surface growth process. At the low and high temperature phases the roughness $W$ grows indefinitely with the time, with growth exponent $\beta_w \simeq 0.50 (W \sim t^{\beta_w})$. At criticality the growth presents a crossover at a characteristic time $t_c$, from a correlated regime (with $\beta_w \neq 0.50$) to an uncorrelated one ($\beta_w \simeq 0.50$). We also calculate the Hurst exponent $H$ of the corresponding surfaces. At criticality, $\beta_w$ and $H$ have values characteristic of correlated growth, distinguishing second- from first-order phase transitions. It has also been shown that the Family-Vicsek relation for the growth exponents also holds for the noise-reduced roughness with an anomalous scaling.

DOI: 10.1103/PhysRevE.75.046106 PACS number(s): 05.50.+q, 02.50.−r, 68.35.Ct, 68.35.Rh

## I. INTRODUCTION

In recent years, the emergence of rough surfaces under far-from-equilibrium conditions has been a central theme in both experimental and theoretical statistical physics [1–3]. The application of self-affine fractals and scaling methods was essential to the progress that has been made towards the understanding of these nonequilibrium phenomena. The standard tools used to describe various self-affine structures observed in disordered surface growth are the roughness $\alpha$, the Hurst $H$, and the growth $\beta_w$ exponents [4–6]. The central goal of this approach is to provide information about the correlations between fluctuations of a space and/or time varying property of the system. Theoretical modeling of self-affine growth processes frequently used some of the models investigated in critical phenomena, e.g., directed percolation and random field Ising [4] and sine-Gordon [7] models.

On the other hand, the inverse problem, i.e., using the roughness exponents to study the main features of the phase diagram of equilibrium spin models, has not been much explored up to now. In 1997, de Sales *et al.* [8] have mapped cellular automata (CA) configurations on solid-on-solid-like profiles and used the Hurst exponent $H$ to classify the elementary Wolfram CA rules. They have also shown that this exponent can be used to detect the frozen-active transition in the one-dimensional Domany-Kinzel CA (DKCA) [8]. Atman *et al.* [9] have also determined the exponent $\beta_w$ for a growth process generated by the spatiotemporal patterns of the DKCA. They have shown that $\beta_w$ presents a cusp at criticality and conjectured that the growth exponent method can be used to detect phase transitions in other models. The advantage of this method to find the phase diagram of the DKCA is that it was not necessary to wait for the system to "thermalize," a process which often expends a lot of computational time. Recently, this method was extended to the Potts and clock models on the square lattice [10] and to the Ising model in $d=1$ with long-range interactions [11]. It has been shown that the Hurst exponent method is able to detect the equilibrium phase transitions and provides accurate numerical determination of the critical temperatures of these models without any reference to thermodynamic potentials, order parameters, or response functions. The procedure used by these authors consists in mapping the spatiotemporal patterns generated by these models to a one-dimensional solid-on-solid particle deposition. At criticality, the scaling properties of the interface can be related to those of the original spin model. Similar methods were also used to study the Edwards-Wilkinson equation with columnar noise [12], sandpile models [13], and also the contact process [14].

We intend here to deepen the application of the surface growth tools to magnetic spin models. The previous works in magnetic spin systems [10,11] have been restricted to the static (Hurst exponent) properties of the one-dimensional mapped interfaces. In this work, we extend this technique, measuring the Hurst and also the growth exponent of two-dimensional surfaces generated by the $q$-state Potts model and the spin-1 Blume-Capel model on the square lattice. These models not only can be applied to real systems [15–18] but also present rich critical behaviors: second- and first- order phase transitions and a tricritical point. Our primary aim is not just to determine the criticality and phase diagrams of the two-dimensional models, since in the literature there are plenty of very accurate methods using, for instance, Monte Carlo simulations [19]. We are mainly interested in obtaining the dynamic critical behavior of their growth surfaces and determining their corresponding universality classes which, from a theoretical point of view is, by itself, important in what concerns the dependence of the critical exponents on the dimensionality. We thus investigate the behavior of the surfaces generated by these models at criticality through the roughness and the exponents $\alpha$, $H$, and $\beta_w$ and compare them with those coming from other one-dimensional realizations.

The plan of this paper is as follows. In Sec. II we describe the models and define the growth process which maps spin

 

configurations into surfaces, as well as the scaling relations expected for the system. In Sec. III, using this mapping, we present numerical results for the growth exponent $\beta_w$ and for the Hurst exponent $H$, which characterize the phase transitions of the $q$-state Potts model and the spin-1 Blume-Capel model on the square lattice. We also discuss the validity of the Family-Vicsek scaling for the noise-reduced roughness $W^*$. Finally, we conclude and indicate future directions of this work in Sec. IV.

## II. MODELS, SIMULATIONS, AND FORMALISM

### A. Models

One of the models of this study is the $q$-state Potts ferromagnet [18,20], consisting of spin variables $\sigma_i$ which may take on $q$ discrete values $\sigma_i=0,1,\ldots,(q-1)$ and are coupled by the dimensionless Hamiltonian

$$-\beta\mathcal{H}_P = K\sum_{\langle ij\rangle}\delta(\sigma_i,\sigma_j), \tag{1}$$

where $\delta(\sigma_i,\sigma_j)$ is the Kronecker delta function [$\delta(\sigma_i,\sigma_j)=1$ when $\sigma_i=\sigma_j$ and $\delta(\sigma_i,\sigma_j)=0$ when $\sigma_i\neq\sigma_j$], the sum runs over all pairs of nearest-neighbor sites in the lattice, $K=J/k_BT$, $k_B$ is the Boltzmann constant, $T$ is the temperature, and $J>0$ is the coupling constant. On the square lattice, in the thermodynamic limit, the $q$-state Potts ferromagnet presents second-order phase transitions with distinct universality classes for $q=2$, 3, and 4 and first-order phase transitions for $q\geqslant 5$ at the transition temperatures $T_c(q)=1/\ln(1+\sqrt{q})$ (in units of $J/k_B$). The $q=2$ Potts model is equivalent to the spin-1/2 Ising model.

The other model we consider is the spin-1 Blume-Capel model [21,22] which can be viewed as a simple generalization of the Ising model where the spin variables $\sigma_i$ may take on the discrete values $\sigma_i=-1,0,1$ and are coupled by the dimensionless Hamiltonian

$$-\beta\mathcal{H}_{BC} = K\sum_{\langle ij\rangle}\sigma_i\sigma_j - \frac{D}{k_BT}\sum_{i=1}^{N}\sigma_i^2, \tag{2}$$

where the first sum here also runs over all pairs of nearest-neighbor sites, $D$ is the single-spin anisotropy parameter, and $N$ is the number of sites. On the square lattice, this model presents a rich phase diagram with ordered ferromagnetic and disordered paramagnetic phases separated by a transition line that changes from an Ising-like continuous phase transition to a first-order transition at a tricritical point located at $k_BT_t/J\simeq 0.609(4)$ and $d_t=D_t/J\simeq 1.965(5)$ [23,24].

### B. Simulations

Here we consider numerical simulations of the models defined above on square lattices with $N=L\times L$ sites submitted to periodic boundary conditions. For updating the spin configurations $\{\sigma_i(t)\}$ we use a single spin-flip Monte Carlo heat bath algorithm.

The surface growth process consists in accumulating (summing) all the values assumed by the variables $\sigma_i(t')$ over the first $t$ Monte Carlo time steps. Specifically, to a unique sequence of spin states $(\{\sigma_i(0)\},\{\sigma_i(1)\},\ldots,\{\sigma_i(t)\})$ corresponds a surface $\{h_i(t)\}$ with the height $h_i(t)$ at site $i$ given by

$$h_i(t) \equiv \sum_{t'=0}^{t}\rho_i(t'), \tag{3}$$

with $\rho_i(t')=\sigma_i(t')$ for the spin-1 Blume-Capel model and $\rho_i(t')=+1$ or $-1$ when $\sigma_i(t')=0$ or 1 for the $q=2$ Potts model, $\rho_i(t')=+1$, 0 or $-1$ when $\sigma_i(t')=0$, 1, or 2 for the $q=3$ Potts model and so on. The model (3) defines a process of the solid-on-solid type, resulting in an aggregate which is compact (no vacancies) and without surface overhangs. The interface advances in time by deposition ($\rho>0$) and evaporation ($\rho<0$) of atoms on the initial substrate. In the low-temperature phases of the spin models we expect that the deposition processes dominate and the interface average height increases with time. At high temperatures, the two processes, deposition and evaporation, take place with equal probability and the velocity of the interface goes to zero. Thus the surface $\{h_i(t)\}$ can be thought of as a driven interface whose dynamics, as we will show, reflects the critical properties of the models.

Our simulations were performed with initial configurations in which all the spins were ordered in the larger spin value [for example, $\{\sigma_i(0)=1\}$ for the Blume-Capel model] and the initial deposit substrate was flat ($\{h_i(0)=0\}$). Although the final results are independent of this initial condition, it is closer to the flat substrate condition in surface growth simulations. The system size in the simulations was changed between $L=32$ and $L=1024$. The maximum Monte Carlo time ranged from about $t=10^2$ to $t=10^5$. To obtain good statistics we took averages over 100–2000 independent runs, depending on the model, the temperature, and the system size.

### C. Formalism

We turn now to the basic scaling analysis of the interface. We characterize the development of the fluctuations of the two-dimensional interface [with heights $h_i(t)$] at time $t$ over a window of size $\epsilon$ by the rms displacement function, or local roughness, $W(\epsilon,t)$ given by

$$W(\epsilon,t) = \sqrt{\langle \overline{h^2} - \bar{h}^2\rangle_i}, \tag{4}$$

where the brackets $\langle\cdots\rangle_i$ denote an average over the window position $i=1,2,\ldots,L^2$. The averages $\bar{h}$ and $\overline{h^2}$ are defined through

$$\bar{f} = \frac{1}{\epsilon^2}\sum_{\vec{r}} f(\vec{r}), \tag{5}$$

with the sum over the positions $\vec{r}$ inside a two-dimensional window of linear size $\epsilon$ centered at site $\vec{r}_i$.

At long times the roughness behaves as [4–6] $W(\epsilon, t\gg t_c)\sim\epsilon^H$ where $t_c$ is a crossover time and $H$ is the Hurst exponent. In this regime the roughness $W(\epsilon,t)$ can distinguish two possible types of profiles. If it is random or even

exhibits a finite correlation length extending up to a characteristic range (such as in a Markov chain), then $W \sim \epsilon^{1/2}$ as in a normal random walk. In contrast, if the self-affine profile has infinitely long-range correlations (no characteristic length), then we expect $H \neq 1/2$.

The scaling ansatz for the global roughness $W(L,t) = W(\epsilon = L,t)$ with respect to time $t$ and the size $L$ is [5,25]

$$W(L,t) \sim L^{\alpha} f\left(\frac{t}{L^{z_w}}\right), \tag{6}$$

where $f(u)$ is a universal scaling function, $\alpha$ is the roughness exponent, $z_w = \alpha/\beta_w$ is the dynamic exponent, and $\beta_w$ is the growth exponent. The function $f(u) = \text{const}$, at long times ($t \gg t_c$), and $f(u) \sim u^{\beta_w}$ at short times ($t \ll t_c$). So, at short times, we expect $W(t) \sim t^{\beta_w}$. At long times, when the lateral (spatial) correlation length of the growth process equals the lattice length $L$, the roughness saturates and behaves as $W(L,\infty) \sim L^{\alpha}$. The crossover time $t_c$ between these two regimes grows as $t_c \sim L^{z_w}$. The particular case in which $W$ does not saturate, growing instead as $W(L,t) \sim t^{1/2}$, corresponds to uncorrelated growth. Thus the exponent $\alpha$ is not defined for this case and $\beta_w = 1/2$. Typically, the exponents $H = \beta_w = 1/2$ are characteristic of the random deposition (RD) growth model, in which a column is randomly chosen along the substrate and a particle is launched vertically until it is deposited at the top of the selected column. In general, $H$ and $\alpha$ are most often the same thing, in particular when the simple Family-Vicsek scaling applies [5,25]. However, $\alpha \neq H$ has been observed in wood [26] and granite fracture surfaces [27].

Equation (3), in fact, defines a model of an aggregate of noninteracting particles deposited or evaporated by correlated mechanisms (the Potts model and Blume-Capel model dynamics). In the present case, away from criticality, the correlation length $\xi$ and correlation time $\tau$ of the spin models are finite, and the corresponding noise in the deposition process is correlated only over short ranges. We expect that in this case, for times greater than $\tau$, the noise appears uncorrelated, and that the RD growth exponents, $H = \beta_w = 1/2$, are verified from the first steps in the growth process.

In contrast, at a continuous phase transition, $\xi$ and $\tau$ diverge and the correlations are long ranged, giving a power law decay of the noise autocorrelation. In this case, the exponents $H$ and $\beta_w^{(c)}$ should deviate from 1/2. From Eq. (3) we can actually estimate the value of the growth exponent $\beta_w^{(c)}$ at a continuous transition temperature $T = T_c$. We get (a similar result was obtained in Refs. [28,9])

$$\beta_w^{(c)} = 1 - \frac{\beta}{\nu z} \quad (L \to \infty), \tag{7}$$

where $\beta$, $\nu$, and $z$ are, respectively, the order parameter ($m(T) \sim |T - T_c|^{\beta}$), correlation length [$\xi(T) \sim |T - T_c|^{-\nu}$], and dynamic critical [$\tau(L) \sim L^z$] exponents of the spin model. For the two-dimensional (2D) Ising universality class, the critical exponent values are $\beta = 1/8$, $\nu = 1$, and, within the heat bath dynamics, $z \simeq 2.17$ [19,29], which results in $\beta_w^{(c)} \simeq 0.942$. For the $q=3$ ($q=4$) Potts model we expect $\beta_w^{(c)} \simeq 0.939$ (0.969) and, at the tricritical point of the Blume-Capel model, $\beta_w^{(c)} \simeq 0.968$ (we have adopted the value of $z = 2.17$, although our results are, within the error bars, also consistent with the exponent $z = 2.198$ from Ref. [29]). At a first-order phase transition there is no long-range correlations and we expect $H = \beta_w = 1/2$ even at $T = T_c$. However, in cases where the order of the transition is difficult to be distinguished in finite systems, these RD values cannot be attained in the simulations. In the $q=5$ Potts model, for example, there is an apparent divergence of the correlation length in the critical region and pseudocritical exponents $\beta \simeq 0.07$ and $\nu \simeq 0.59$ can be defined [30]. By assuming the validity of Eq. (7) in this case, we obtain $\beta_w^{(c)} \simeq 0.945$.

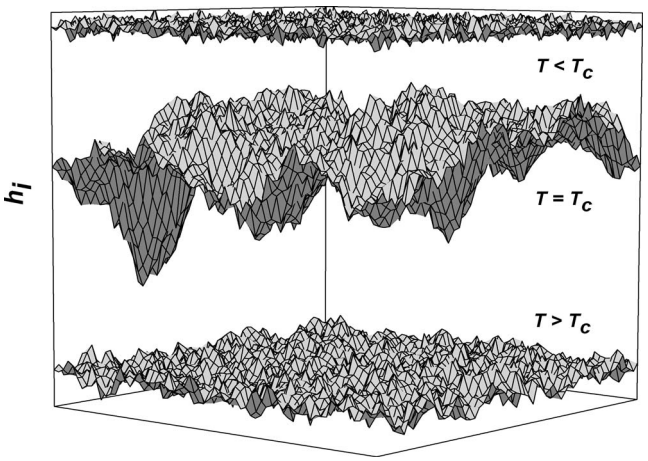


FIG. 1. Some typical interfaces obtained from equilibrium spin configurations of the $q=2$ Potts model (Ising model) on the square lattice with $L=64$ at the temperatures $T=0.1345$, $T=1.1345 \simeq T_c$, and $T=2.1345$.

## III. RESULTS

In what follows the temperature $T$ is measured in units of $J/k_B$. Figure 1 shows typical snapshots of the surfaces generated by equilibrium spin configurations of the $q=2$ Potts model (Ising model) on the square lattice with $L=64$. For $T \neq T_c$ we observe that the surfaces appear rough down to short length scales, whereas for $T \simeq T_c$ the surface presents large fluctuations.

In Fig. 2 we show some plots of the roughness $W$ as a function of temperature at large arbitrary fixed times (of order $2 \times 10^4$) and system sizes $L=32$ and $L=64$, exhibiting peaks at temperatures $T_w$ around the critical temperatures of the corresponding spin models. These results correspond to averages over typically $M=200$ samples. We show curves for the $q=2$, 3, 7, and 10 Potts model and the Blume-Capel model with different anisotropy parameter values ($d=D/J$), including the tricritical one $d_t$. We also observe that as we increase the system size the peaks in $W$ increase and become sharper. For all the first-order transitions and the tricritical point of the Blume-Capel model the curves exhibit cuspid-like shapes.

From $T_w$, at which $W$ exhibits a peak, it is possible to obtain the transition temperatures of the system in the ther-

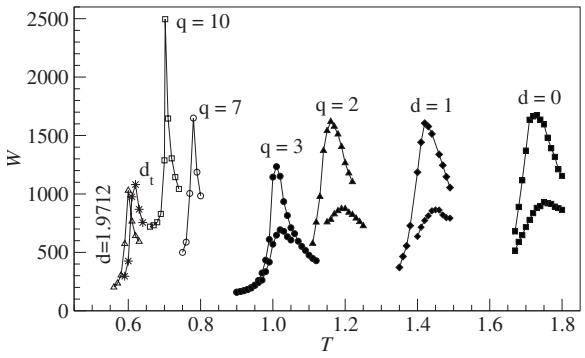


FIG. 2. The roughness $W$ as a function of temperature at large arbitrary fixed times and sizes $L=64$ (for $q=2$, 3, 7, and 10 Potts model and the Blume-Capel model with different anisotropy parameters $d=D/J$, including the tricritical one $d_t$) and $L=32$ (lower curves shown only for $q=2$, $q=3$, $d=1$, and $d=0$).

modynamic limit. The usual finite-size scaling approach provides in this case first- and second-order transition lines which are in good agreement with the exact (or previous approximated) values of the corresponding models (they agree, within the error bars, with those from Refs. [23,24] for the Blume-Capel model).

### A. Growth exponent $\beta_w$

The curves shown in Fig. 2 are for fixed sizes and time. For a fixed size $L$, as the time increases, the roughness $W$ grows indefinitely for any non-null temperature, which is characteristic of an asymptotic uncorrelated dynamics. Similar results were obtained for a probabilistic cellular automaton [28] and for the contact process [14] where the saturation of $W$ can be observed only if the averages include the samples which reach the absorbing state (in which the interface is pinned and $W$ remains fixed) exhibited in these systems. At temperatures away from criticality, the roughness is independent of the system size $L$ and the fitted straight lines to the data show that, after a fast transient, the roughness increases with $\beta_w \simeq 0.50$, characteristic of uncorrelated

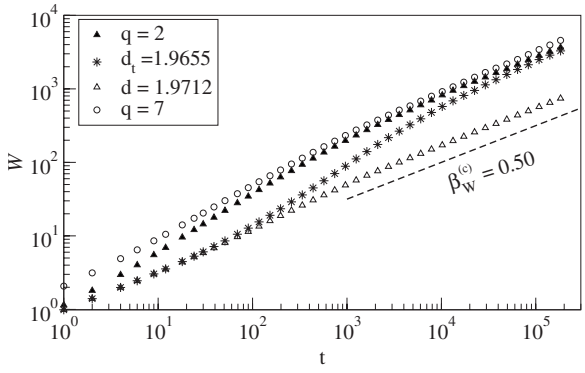


FIG. 3. Log-log plot of the roughness $W$ vs time $t$ at $T \simeq T_c$ for different models and $L=64$. The dashed line is a guide for $\beta_w = 0.50$. The curves are for the $q=2$ and $q=7$ Potts model and for the Blume-Capel model with $d=1.9712$ and $d \simeq d_t$. The error bars are smaller than the symbol sizes.

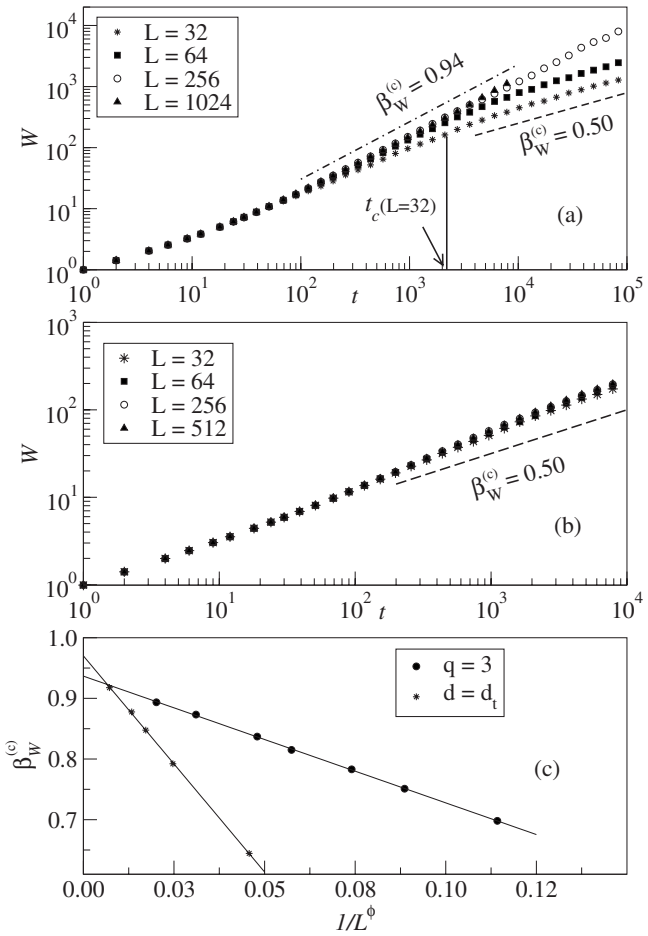


FIG. 4. (a) Log-log plot of the roughness $W$ vs time $t$ at $T \simeq T_c$ for the $q=2$ Potts model with various values of $L$. The arrow indicates the characteristic time $t_c$ according to the text. (b) The same as in (a) but for the Blume-Capel model with $d=1.9752$. (c) Extrapolation of $\beta_w^{(c)}$ vs $L^{-\phi}$ for the $q=3$ ($\phi=0.626$) Potts model and for the Blume-Capel model with $d \simeq d_t$ ($\phi=0.89$).

growth. The situation is, however, quite different at $T_c$. In Fig. 3 we show double logarithmic plots of the roughness $W$ vs time $t$ for the $q=2$ and $q=7$ Potts model and for the Blume-Capel model with $d=1.9712$ and $d \simeq d_t$ at their transition temperatures. We observe, in general, for $T \simeq T_c$, the existence of two distinct linear portions in the curves of $W$, whose intersection point defines a size dependent characteristic time $t_c(L)$. This crossover defines two straight lines, one for long times, with the same slope as for $T$ far from $T_c$, $\beta_w \simeq 0.50$, and another one for $t < t_c$, with $\beta_w^{(c)} > 0.50$ characteristic of correlated growth. The data used to determine $\beta_w^{(c)}$ were then obtained for short times ($t < 10^3$) and $M=2000$ samples. At the second-order transitions we observed a significant dependence of the values of $\beta_w^{(c)}$ with the system size, as can be seen in Fig. 4(a) for the $q=2$ Potts model. At the first-order transitions this dependence of $\beta_w^{(c)}$ on $L$ is very weak, as can be seen in Fig. 4(b) for the Blume-Capel model with $d=1.9752$. We have thus extrapolated the data of $\beta_w^{(c)}$ for $1/L \to 0$ and obtained values which, at the second-order transitions, agrees well with the values predicted by scaling arguments, according to Eq. (7). Some examples of the esti-

TABLE I. Summary of the exponents $\beta_w^{(c)}$ and $H$ for the $q$-state Potts model ($P_q$) and for the Blume-Capel model ($BC_d$). The values in the second column are the results coming from Eq. (7) and those in the third and fourth columns are from the present simulations. The exponents $H$ for $q=10$ and $d=1.9878$ are quite difficult to be obtained because the roughness saturates very fast as a function of $\epsilon$ ($\epsilon^* \to 0$). The exponents are also shown for directed percolation (DP), contact process (CP), and Domany-Kinzel cellular automata (DKCA) universality classes in $d=1+1$ dimensions according to [9].

| Model | $\beta_w^{(c)}$ | $\beta_w^{(c)}$ | $H$ |
|---|---|---|---|
| $P_{q=2}$ | 0.942… | 0.945(4) | 0.725(6) |
| $P_{q=3}$ | 0.939… | 0.937(1) | 0.730(4) |
| $P_{q=4}$ | 0.969… | 0.970(6) | 0.735(5) |
| $P_{q=5}$ | 0.945… | 0.941(1) | 0.714(5) |
| $P_{q=6}$ | | 0.830(6) | 0.626(8) |
| $P_{q=7}$ | | 0.800(1) | 0.50(1) |
| $P_{q=10}$ | | 0.699(4) | |
| $BC_{d=0}$ | 0.942… | 0.950(8) | 0.715(6) |
| $BC_{d=1.95}$ | 0.942… | 0.946(7) | 0.703(7) |
| $BC_{d_t=1.9655}$ | 0.968… | 0.970(3) | 0.709(5) |
| $BC_{d=1.9712}$ | | 0.820(7) | 0.468(5) |
| $BC_{d=1.9878}$ | | 0.501(2) | |
| DP | | 0.8405 | 0.643 |
| CP | | 0.839(1) | 0.63(3) |
| $DKCA_{p_2=0.5}$ | | 0.82(2) | 0.61(3) |
| $DKCA_{p_2=1.0}$ | | 0.99(1) | 0.99(2) |
| $DKCA_{p_1=1.0}$ | | 0.81(1) | 0.60(3) |
| $DKCA_{p_2=0}$ | | 0.78(2) | 0.61(3) |

mate of $\beta_w^{(c)}$ for $1/L \to 0$ are shown in Fig. 4(c). The numerical results are given in Table I and are also plotted in Fig. 5. The exponent $\phi$ in Fig. 4(c) has been adjusted in order to get the minimum $\chi^2$ in the corresponding linear fittings (these finite-size corrections to the exponent $\beta_w$ are just *ad hoc* guesses, and we are not aware of any better scheme for such extrapolation).

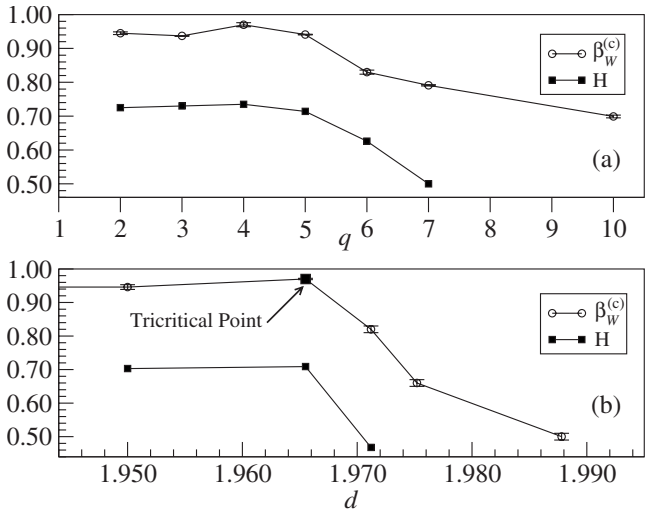


FIG. 5. Growth exponent $\beta_w^{(c)}$ and Hurst exponent $H$ vs (a) the number of states $q$ of the Potts model and (b) the anisotropy parameter $d$ of the spin-1 Blume-Capel model.

At a first-order phase transition there are no long-range correlations developing and we should expect $\beta_w^{(c)}=1/2$. However, some models can present very large correlation length and correspondingly large critical slowing down at the transition and the true first-order behavior can only be caught for very large lattice sizes. In the $q=5$ Potts model, for example, the estimated correlation length is of order of 2000 lattice spacings and the pseudocritical exponents $\beta \simeq 0.07$ and $\nu \simeq 0.59$ [30] lead to a prediction of $\beta_w^{(c)}=0.945$ which, even in this case, agrees very well with the obtained numerical value 0.941(1). From Table I we can note that a $\beta_w^{(c)} \neq 1/2$ is also obtained for $q=6,7$, and $q=10$ and $d=1.9712$ (we are not aware, in these cases, of any pseudocritical exponent to compare with), meaning that our limited system sizes do not attain the correct value $\beta_w^{(c)}=1/2$ in the thermodynamic limit. However, as can be seen in Fig. 5, our results show that for increasing values of $q$ in the Potts model and $d$ in the Blume-Capel model, the exponents $\beta_w^{(c)}$ approach indeed the expected value 1/2, corresponding to uncorrelated growth. We can also see that for the second-order transitions there is a quite good agreement of the extrapolated values to those coming from the scaling relation (7).

To determine the crossover time $t_c(L)$ we measured the intersection of the two fitted lines, one with $\beta_w=\beta_w^{(c)}(L)$ for short times and the other with $\beta_w \simeq 0.5$ for long times, as shown by the arrow in Fig. 4(a) for $q=2$. The maximum size in which we studied this crossover was $L=256$ due to the large computational demand necessary, in some cases, to observe the $\beta_w \simeq 0.50$ regime. At the second-order transitions we obtained that $t_c \sim L^{z_1}$ with the values of the exponent $z_1$ agreeing with the value of the dynamic critical exponent $z$ of the spin model within the heat bath dynamics. At the first-order transitions we obtained curves for $t_c(L)$ which saturate as $L$ increases.

We can understand the crossover (shown in Fig. 3) in the roughness dynamics at $T_c$ as a consequence of the decay of the long-ranged correlations in the spin models at criticality. In this sense the characteristic time $t_c$ seems to be a measure of the finite-size relaxation time $\tau$ of the spin models dynamics at criticality, in support to the fact that we observed $z_1 \simeq z$.

### B. Hurst exponent *H*

In order to characterize the spatial correlations in the grown surfaces at the equilibrium regime ($\beta_w^{(c)} \simeq 0.5$) of the spin models, we calculated the local exponent $H$ at times greater than $t_c$. Contrary to what happens in obtaining the growth exponent, in this case the procedure is much more time consuming. We have considered here $t=2\times10^5$ and $M=200$ samples. As an example, Fig. 6 shows log-log plots of the local roughness $W$ vs the window size $\epsilon$ for the Blume-Capel model at the tricritical point (a) and for the $q=7$ Potts model at the first-order transition (b). The power-law portions of the curves, before the saturation regime, yields the Hurst exponent $H$, which in these cases give $H$

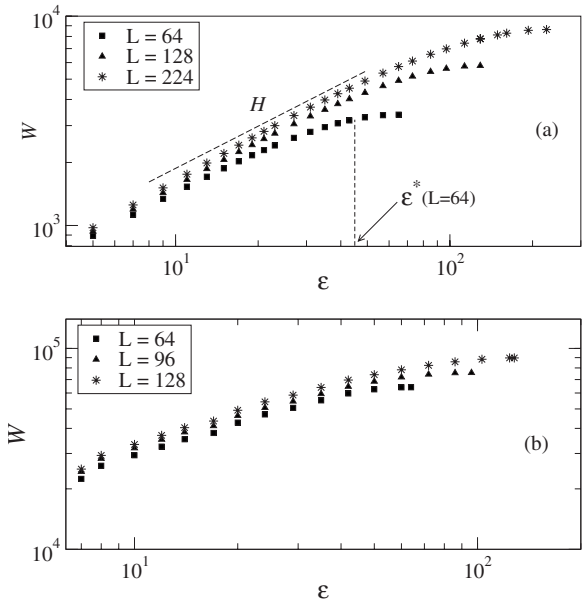


FIG. 6. Log-log plot of the roughness $W$ at times greater than $t_c$ vs window size $\epsilon$ for (a) the Blume-Capel model with $d \simeq d_t$ and (b) the $q=7$ Potts model. The error bars are smaller than the symbol sizes.

$=0.709(5)$ and $H=0.50(1)$, respectively. Similar behavior is obtained for other values of $q$ and $d$, whose values are given in Table I and depicted in Fig. 5, where one can clearly see that the local Hurst exponent reaches the expected value $H=1/2$ much faster than the growth exponent.

The values of the local roughness $W(\epsilon)$ seems to be a measure of the average size of the spin islands or magnetized domains limited by the correlation length $\xi$. In this sense, the exponent $H$ is a measure of the local spatial correlations at the phase transitions. In fact, at continuous phase transitions we obtained $H \simeq 0.7$, reflecting the long-range correlations, while at the first-order transitions we obtained $H \simeq 1/2$. We also observed that the crossover length $\epsilon^*(L)$ between the power-law portions of the curves of $W(\epsilon)$ and the saturation regime [see Fig. 6(a)] grows as a power law $\epsilon^*(L) \sim L^x$ (with $x \simeq 1$) for the second-order transitions and tricritical point and saturates to a finite value at the first-order transitions. This saturation of $\epsilon^*$ is hard to be seen in the very weak first-order transitions but is very fast in the other cases. For the $q=10$ Potts model and for the Blume-Capel model with $d=1.9878$, for example, $\epsilon^*$ is of order of only ten lattice spacings and the estimates of the local exponent $H$ are quite difficult. The saturation of $\epsilon^*(L)$ for a small finite value at the thermodynamic limit is also observed in all models at temperatures away from $T_c$.

### C. Family-Vicsek and anomalous scalings

The fact that the roughness $W$ grows indefinitely as time increases, even at the second-order critical temperatures, as can be seen in Fig. 3, is related to the intrinsic noise in the Monte Carlo algorithms. After the transients, the systems follow a random walk in the phase space, adding a Gaussian noise to the temporal behavior of the mapped surface roughness $W$. This noise gives a diffusive factor in the thermal averages, resulting in the asymptotic $t^{1/2}$ behavior. This means that $\alpha \to \infty$ and that the Family-Vicsek scaling (6), namely $z_w = \alpha/\beta^w$, is no longer valid. A way to extract the effect of the intrinsic noise from $W$, and to study the evolution of the roughness without this trivial growing, can be done by defining the new roughness $W^*$ such that

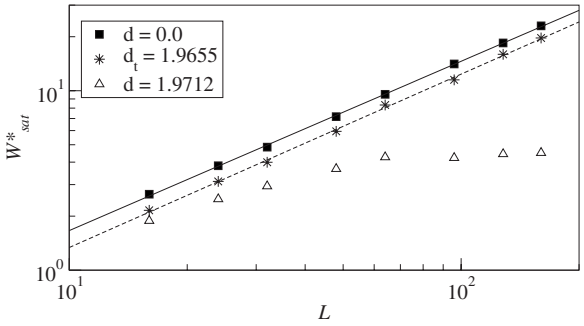


FIG. 7. Log-log plot of the saturation values of the noise-reduced roughness $W^*$ as a function of $L$. The data are for the Blume-Capel model with $d=0$, $d=1.9172$, and $d \simeq d_t$. The error bars are smaller than the symbol sizes.

$$W(\epsilon,t) = t^{1/2} W^*(\epsilon,t). \tag{8}$$

So, the noise-reduced roughness $W^*(\epsilon,t)$ should have a behavior similar to regular surface growing processes, scaling as $W^*(\epsilon, t \gg t_c) \sim \epsilon^{H^*}$, at short times as $W^*(t) \sim t^{\beta_w^*}$, and at long times as $W^*(L,\infty) \sim L^{\alpha^*}$, where also $t_c \sim L^{z_w^*}$. It means that for $t \gg t_c$ and for a given $L$, $W^*$ is a constant and the time behavior of $W \sim t^{1/2}$ is preserved. We expect that $H^*=H$, $z_w^*=z$, $\beta_w^*=\beta_w-0.5$, and $\alpha^*$ can now be obtained through the graphs of $W^*(L,\infty)$ vs $L$. In Fig. 7 we show typical examples of the saturated value of $W^*$ as a function of the system size $L$. We observed that for the first-order transitions the curves of $W^* \times L$ saturate, which results in $\alpha^*=0$ at the thermodynamic limit. This is consistent with a finite correlation length in these cases. At the tricritical point and second-order phase transitions, the fitted straight lines yield the roughness exponent $\alpha^*$. From this we can show that the Family-Vicsek scaling [Eq. (6)] holds for these cases, with $\alpha^*$ in place of $\alpha$ and $z_w=\alpha^*/\beta_w^*$. For instance, for the Blume-Capel model at $d=0$ we have, from Table I, $\beta_w^*=0.942-0.5=0.442$. This gives $\alpha^*=z\beta_w^*=0.959$, which is comparable to the measured value $\alpha^*=0.954(7)$ from Fig. 7. Similar results are obtained for other second-order transitions, including the Potts model. At the tricritical point we have $\alpha^*=z\beta_w^*=1.02$, suggesting that this transition may lead to a surface with super-roughening behavior (the term super-roughening has been used when the global exponent $\alpha^*>1$).

A log-log plot of the noise-reduced roughness $W^*$ as a function of time $t$ for the Blume-Capel model with $d=0$ is shown in Fig. 8. The inset in this figure shows these same data collapsed for $\alpha^*=0.954(7)$ and $z=2.17$. The collapse fails for short times because the system is still uncorrelated. We also observed that at the second-order transitions the local roughness exponent $H$ is different (smaller) from the global value $\alpha^*$ which means that the surfaces are not self-

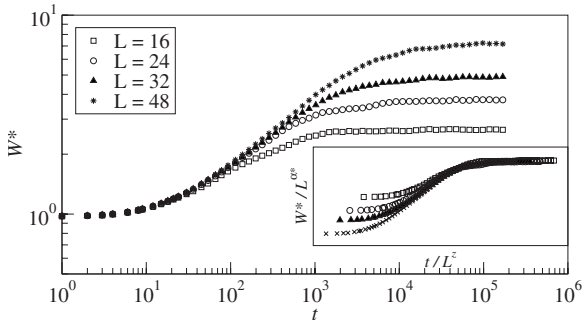


FIG. 8. Log-log plot of the noise-reduced roughness $W^*$ as a function of time $t$ for the Blume-Capel model with $d=0$. Inset shows this same data collapsed for $\alpha^*=0.954(7)$ and $z=2.17$.

affine. Since the local and global surface fluctuations have different scaling exponents, the noise-reduced roughness presents intrinsic anomalous scaling [27,31,32]. For example, for the Ising universality class we obtained $\alpha^*=0.954(7)$ while $H\simeq 0.72$, for the Blume-Capel model with $d\simeq d_t$ we obtained $\alpha^*=0.98(2)$ while $H=0.709(5)$. This fact is consistent with the idea that at the continuous transitions the correlations in the spin models are distinct at large and small length scales. As expected, for first-order transitions the anomalous scaling is stronger than for second-order ones (note that in this case one has $\alpha^*=0$ and $H\simeq 0.5$).

## IV. CONCLUSIONS

Defining a growth model based on the dynamics of the $q$-state Potts model and of the spin-1 Blume-Capel model on the square lattice, we have studied the phase transitions in these systems through the roughness technique.

We have shown that the growth surfaces exhibit distinct characteristic dynamics, measured by the growth exponent $\beta_w$, and local spatial correlations, measured by the Hurst exponent $H$. For $T\neq T_c$ the growth is always uncorrelated and $\beta_w\simeq 0.50$ and $H\simeq 0.50$. At $T\simeq T_c$ the roughness presents a crossover from a correlated regime ($t<t_c$) to an uncorrelated one ($t>t_c$). At this crossover the growth exponent changes from a value $\beta_w^{(c)}>0.50$ to $\beta_w\simeq 0.50$. The crossover time $t_c$ is a measure of the finite-size relaxation time $\tau$ of the spin models at $T_c$.

For a fixed time $t\gg t_c$, the roughness $W$ has sharp peaks at temperatures $T_w$, whose extrapolated values agree well with the static critical temperatures of the spin models on the square lattice. The peaks are rounded at the second-order and cuspidlike at the first-order phase transitions and at the tricritical point.

The results of this study point out that one can determine the order of the transition, the critical temperature, as well as static and dynamic critical exponents of spin models through the same scaling methods applied to surface growth phenomena. Our results for the Hurst exponent at equilibrium ($t\gg t_c$) are consistent with long-range correlations ($H\simeq 0.7$) at the second-order and short-range correlations ($H\simeq 0.5$) at the first-order phase transitions. Although the present approach is restricted to the Potts and Blume-Capel models on the square lattice, we believe that our results can be extended to any transition observed in lattice spin models.

From Table I one can note that the dynamic and static surface exponents ($\beta_w$ and $H$) for $q=2$, $d=0$, and $d=1.95$ (i.e., second-order phase transitions) agree within the error bars, being in the same universality class, as expected. For $q=3$, $q=4$, and at the nonclassical tricritical point, the exponents are different and in agreement with Eq. (7). However, in this case, the values for the exponents seem not to change quite as much from different universality classes. The change in the exponents are, nevertheless, clear when compared to the one-dimensional versions of surface growth, shown in Table I for directed percolation (DP), contact process (CP), and Domany-Kinzel cellular automata (DKCA) universality classes in $d=1+1$ dimensions, according to [9].

The Family-Vicsek relation holds for the noise-reduced roughness $W^*$ with an intrinsic anomalous scaling, characteristic of surfaces which are not self-affine.

We have chosen to apply the growth exponent method to these spin models because they are prototypes of statistical mechanical systems exhibiting second- and first-order phase transitions and also a tricritical point. Although they were originally proposed as simple models of ferromagnetic systems, today they have been applied to a diverse range of phenomena such as the freezing and evaporation of liquids, the folding of proteins, social networks, neural networks, and glassy substances. Thus the results found here might be helpful in future investigations of these phenomena.

Another problem we can address using this roughness method is the study of phase transitions of the Kosterlitz-Thouless type, such as that which occurs in the $XY$ model on the square lattice. Also, the universality of two-dimensional disordered spin models, in which the Harris conjecture fails [33], could also be addressed by this approach. We intend to examine these questions in a future work.

## ACKNOWLEDGMENTS

We thank the Brazilian agencies $CNP_q$ and Fapemig for financial support of this work. We thank also Albens P. F. Atman and J. G. Moreira for fruitful discussions.

[1] N. M. Hasan, J. J. Mallett, S. G. dos Santos Filho, A. A. Pasa, and W. Schwarzacher, Phys. Rev. B **67**, 081401(R) (2003).

[2] S. O. Ferreira and S. C. Ferreira, Jr., Braz. J. Phys. **36**, 294 (2006).

[3] J. M. Lopez, M. Castro, and R. Gallego, Phys. Rev. Lett. **94**, 166103 (2005).

[4] A. L. Barabási and H. E. Stanley, in *Fractal Concepts in Surface Growth* (Cambridge University Press, Cambridge, En-

gland, 1995).
[5] *Dynamics of Fractal Surfaces*, edited by F. Family and T. Vicsek (World Scientific, Singapore, 1991).
[6] P. Meakin, in *Fractals, Scaling and Growth far from Equilibrium* (Cambridge University Press, Cambridge, England, 1998).
[7] J. Toner and D. P. DiVincenzo, Phys. Rev. B **41**, 632 (1990).
[8] J. A. de Sales, M. L. Martins, and J. G. Moreira, Physica A **245**, 461 (1997); J. Phys. A **32**, 885 (1999).
[9] A. P. F. Atman, R. Dickman, and J. G. Moreira, Phys. Rev. E **66**, 016113 (2002).
[10] J. A. Redinz and M. L. Martins, Phys. Rev. E **63**, 066133 (2001).
[11] A. F. Brito and J. A. Redinz, Physica A **333**, 269 (2004).
[12] K. B. Lauritsen and M. Alava, e-print cond-mat/9903346.
[13] A. Vespignani, R. Dickman, M. A. Muñoz, and S. Zapperi, Phys. Rev. E **62**, 4564 (2000).
[14] R. Dickman and M. A. Muñoz, Phys. Rev. E **62**, 7632 (2000).
[15] S. Kobe, Braz. J. Phys. **30**, 649 (2000).
[16] D. P. Belanger, Braz. J. Phys. **30**, 682 (2000).
[17] W. P. Wolf, Braz. J. Phys. **30**, 794 (2000).
[18] F. Y. Wu, Rev. Mod. Phys. **54**, 235 (1982).
[19] D. P. Landau and K. Binder in *A Guide to Monte Carlo Simulations in Statistical Physics* (Cambridge University Press, Cambridge, England, 2000).
[20] R. B. Potts, Proc. Cambridge Philos. Soc. **106**, 48 (1952).
[21] M. Blume, Phys. Rev. **141**, 517 (1966).
[22] H. W. Capel, Physica (Amsterdam) **32**, 966 (1966).
[23] J. C. Xavier, F. C. Alcaraz, D. Pena Lara, and J. A. Plascak, Phys. Rev. B **57**, 11575 (1998).
[24] C. J. Silva, A. A. Caparica, and J. A. Plascak, Phys. Rev. E **73**, 036702 (2006).
[25] F. Family and T. Vicsék, J. Phys. A **18**, L75 (1985).
[26] S. Morel, J. Schmittbuhl, J. M. Lopez, and G. Valentin, Phys. Rev. E **58**, 6999 (1998).
[27] Juan M. Lopez and Jean Schmittbuhl, Phys. Rev. E **57**, 6405 (1998).
[28] P. Bhattacharyya, Int. J. Mod. Phys. C **10**, 165 (1999).
[29] L. Schülke and B. Zheng, Phys. Lett. A **204**, 295 (1995).
[30] P. Peczak and D. P. Landau, Phys. Rev. B **39**, 11932 (1989).
[31] Juan M. Lopez and Miguel A. Rodriguez, Phys. Rev. E **54**, R2189 (1996).
[32] Juan M. Lopez, Miguel A. Rodriguez, and Rodolfo Cuerno, Phys. Rev. E **56**, 3993 (1997).
[33] F. W. S. Lima and J. A. Plascak, Braz. J. Phys. **36**, 660 (2006).